

Qubit relaxation from evanescent-wave Johnson noise

Luke S. Langsjoen, Amrit Poudel, Maxim G. Vavilov, and Robert Joynt
Department of Physics, University of Wisconsin, Madison, Wisconsin 53706, USA

(Received 22 March 2012; published 5 July 2012)

In many quantum computer architectures, the qubits are in close proximity to metallic device elements. Metals have a high density of photon modes, and the fields spill out of the bulk metal because of the evanescent-wave component. Thus thermal and quantum electromagnetic Johnson-type noise from metallic device elements can decohere nearby qubits. In this Rapid Communication we use quantum electrodynamics to compute the strength of this evanescent-wave Johnson noise as a function of distance z from a metallic half space. Previous treatments have shown unphysical divergences at $z = 0$. We remedy this by using a proper nonlocal dielectric function. Decoherence rates of local qubits are proportional to the magnitude of electric or magnetic correlation functions evaluated at the qubit position. We present formulas for the decoherence rates. These formulas serve as an important constraint on future device architectures. Comparison with single-electron spin relaxation measurements shows that evanescent-wave Johnson noise may constitute the dominant relaxation mechanism in experiments performed at low magnetic field.

DOI: [10.1103/PhysRevA.86.010301](https://doi.org/10.1103/PhysRevA.86.010301)

PACS number(s): 03.67.-a, 03.65.Yz, 42.50.Lc, 73.21.-b

Qubits with long relaxation times are necessary for quantum computation. Most such devices are controlled electrically. This creates a control-isolation dilemma: connections from the outside world are what make the devices useful, but they are also sources of decoherence. In particular, one may wish to place charge or spin qubits close to metallic device elements used to confine or control the qubits.

The relaxation of a charge or spin qubit can be induced by the thermal and quantum fluctuations of electromagnetic fields. The fluctuations of the electromagnetic fields are greatly enhanced in the vicinity of conductors because of the evanescent waves [1–6]. This evanescent-wave Johnson noise (EWJN) has been shown, both theoretically [7] and experimentally [8], to be an important source of decoherence for atomic qubits near the metallic walls of a trap. In this work we investigate the effects of metallic device elements in solid-state qubit architectures. Similar investigations have been carried out previously using lumped-circuit calculations of Johnson noise [9–11]. Here we do the noise calculations taking into account the detailed spatial dependence of the fields and the important effects of nonlocal corrections to the electromagnetic response functions [12,13].

We pause here to mention that the EWJN originates from properties of the metal near its surface. The expressions for the electromagnetic-field fluctuations presented in this Rapid Communication are for a conducting half space. However, our treatment can be extended to calculate the strength of EWJN in the vicinity of a conducting slab of finite thickness. In this case, the electromagnetic fluctuations are independent of the thickness of the slab as long as this thickness is significantly larger than the skin depth of the metal. As such, we anticipate that EWJN may be alternatively interpreted as arising from overdamped surface plasmon excitations which exist within a skin depth of the surface of the metal [6].

To describe the decoherence of qubits resulting from the evanescent electromagnetic fields surrounding a conducting gate, it is necessary to compute spectral densities of the electric- and magnetic-field fluctuations. Fermi's golden rule and the fluctuation-dissipation theorem imply that the relaxation rate $1/T_1$ of a (charge and spin, respectively) qubit

transition of a particular frequency will be proportional to the spectral densities at that frequency. Specifically, the relaxation time T_1 of a charge qubit with dipole moment \vec{d} pointing in the i th direction at position \vec{r} and level separation ω_Z will be given by

$$\frac{1}{T_1} = \frac{d^2}{\hbar^2} \chi_{ii}^E(\vec{r}, \vec{r}, \omega_Z) \coth\left(\frac{\hbar\omega_Z}{2k_B T}\right), \quad (1)$$

and T_1 of a spin qubit with magnetic dipole moment $\vec{\mu}$ in the i th direction at position \vec{r} and level separation ω_Z will be given by

$$\frac{1}{T_1} = \frac{\mu^2}{\hbar^2} \chi_{ii}^B(\vec{r}, \vec{r}, \omega_Z) \coth\left(\frac{\hbar\omega_Z}{2k_B T}\right), \quad (2)$$

where $\chi_{ii}^{E,(B)}(\vec{r}, \vec{r}, \omega_Z)$ are the electric and magnetic spectral densities, respectively. We deal first with fields that have been averaged over distances of the order of a and l , where a is an interatomic distance and l is the mean free path in the metal. As a result the dielectric function $\epsilon(\vec{r}, \omega)$ may be treated as a local function of space. This approximation breaks down in the near vicinity of the conducting surface, and the influence of a nonlocal dielectric response on the correlation function is addressed below. The conducting electrodes in semiconductor qubit architectures are commonly constructed of copper. Therefore, all numerical results presented here use the electronic properties of copper near 0 K. In this case, a local dielectric function may be used for distances much larger than the Fermi wavelength $\lambda_F = \sqrt{4\pi^2\hbar^2/mE_F} \approx 0.4$ nm. We work in a gauge where the scalar potential $\phi = 0$, so that for harmonic fields we have $\vec{E} = i\omega\vec{A}/c$.

The spectral densities can be shown [6,14] to be directly related to the imaginary part of the equilibrium retarded photon Green's function by the relations

$$\chi_{ij}^E(\vec{r}, \vec{r}', \omega) = \frac{\omega^2}{\epsilon_0 c^2} \text{Im} D_{ij}(\vec{r}, \vec{r}', \omega), \quad (3a)$$

$$\chi_{ij}^B(\vec{r}, \vec{r}', \omega) = \frac{1}{\epsilon_0 c^2} \epsilon_{ikm} \epsilon_{jnp} \partial_k \partial_n \text{Im} D_{mp}(\vec{r}, \vec{r}', \omega), \quad (3b)$$

where i, j are Cartesian indices that run over x, y, z and D_{ij} satisfies

$$\begin{aligned} & \left[-\delta_{ij} \left(\nabla^2 + \frac{\omega^2 \epsilon(\vec{r}, \omega)}{c^2} \right) + \partial_i \partial_j \right] D_{ik}(\vec{r}, \vec{r}') \\ & = -4\pi \hbar \delta^3(\vec{r} - \vec{r}') \delta_{jk}. \end{aligned} \quad (4)$$

The geometry of a particular problem is expressed through the function $\epsilon(\vec{r}, \omega)$. Equations (1) and (2) assume the charge or spin qubit can be adequately approximated as a point dipole. The effect of a qubit with an extended spatial distribution will be considered in future work. The task of computing D_{ij} in a particular geometry is, in general, a complicated problem in electrodynamics. In this Rapid Communication we shall limit ourselves to the situation where the separation of the qubit from the metal surface is much less than any radius of curvature of the surface so that the surface can be thought of as flat.

Let z be the distance from the surface. The result for the spectral density of the electric field for local electrodynamics has been obtained by Henkel *et al.* [7]:

$$\begin{aligned} \chi_{xx}^E(z, z, \omega) &= \frac{\hbar}{2\epsilon_0} \text{Re} \int_0^\infty \frac{p dp}{q} e^{2iqz} \\ & \times \left(\frac{\omega^2}{c^2} r_s(p) - q^2 r_p(p) \right), \end{aligned} \quad (5a)$$

$$\chi_{zz}^E(z, z, \omega) = \frac{\hbar}{\epsilon_0} \text{Re} \int_0^\infty \frac{p^3}{q} dp e^{2iqz} r_p(p), \quad (5b)$$

where $q = \sqrt{\omega^2/c^2 - p^2}$ for $p^2 \leq \omega^2/c^2$ and $q = i\sqrt{p^2 - \omega^2/c^2}$ for $p^2 > \omega^2/c^2$ is the z component of the wavevector and p is the transverse component. Our notation follows that of Ford and Weber [12].

$$r_s(p) = \frac{q - \sqrt{\omega^2 \epsilon/c^2 - p^2}}{q + \sqrt{\omega^2 \epsilon/c^2 - p^2}} \quad (6a)$$

and

$$r_p(p) = \frac{\epsilon q - \sqrt{\omega^2 \epsilon/c^2 - p^2}}{\epsilon q + \sqrt{\omega^2 \epsilon/c^2 - p^2}} \quad (6b)$$

are the Fresnel reflection coefficients. The corresponding expressions for the spectral densities of the magnetic field are identical to Eqs. (5) if we multiply by $1/c^2$ and make the replacement $r_s \leftrightarrow r_p$.

We are interested in separations that are sufficiently small so that retardation and hence radiation of the electromagnetic field may be neglected. This is known as the quasistatic approximation, and it is formally employed by taking the limit $c \rightarrow \infty$. This results in the greatly simplified expressions

$$\chi_{zz}^E(z, z, \omega) = 2\chi_{xx}^E(z, z, \omega) = \frac{\hbar}{8\epsilon_0 z^3} \text{Im} \frac{\epsilon - 1}{\epsilon + 1}, \quad (7a)$$

$$\chi_{zz}^B(z, z, \omega) = 2\chi_{xx}^B(z, z, \omega) = \frac{\hbar \omega^2}{8\epsilon_0 c^4 z} \text{Im}(\epsilon - 1). \quad (7b)$$

Employing this approximation has eliminated the functional difference between the transverse and longitudinal components of the field fluctuations. The quasistatic expressions differ from the exact values by less than 1% when $z < \delta/10$, where δ is the skin depth of the metal. For copper near

absolute zero, $\delta \sim 3 \mu\text{m}$. Equations (7) diverge as $z \rightarrow 0$, but this divergence is not physical: it is an artifact of treating the dielectric function as local at distances comparable to the interatomic spacing. In any differential equation satisfied by the spatial Fourier components of D_{ij} , a local dielectric function will be independent of the wavevector, while a nonlocal one will have a nontrivial wavevector dependence. It is conventional to represent the spatial Fourier components of the nonlocal dielectric function as a tensor quantity in the form

$$\epsilon_{ij}(\vec{k}, \omega) = \epsilon_l(k, \omega) \frac{k_i k_j}{k^2} + \epsilon_t(k, \omega) \left(\delta_{ij} - \frac{k_i k_j}{k^2} \right), \quad (8)$$

where we have separated the function into its longitudinal ϵ_l and transverse ϵ_t components.

Nonlocality in the dielectric function changes the reflection coefficients. In the quasistatic approximation r_p is [12]

$$r_p = \frac{1 - \epsilon_0 \frac{2p}{\pi} \int_0^\infty d\kappa \frac{1}{k^2 \epsilon_l(k, \omega)}}{1 + \epsilon_0 \frac{2p}{\pi} \int_0^\infty d\kappa \frac{1}{k^2 \epsilon_t(k, \omega)}}, \quad (9a)$$

and r_s becomes

$$r_s = \frac{\omega^2}{4p^2 c^2} \left(\frac{4p^3}{\pi \epsilon_0} \int_0^\infty \frac{\epsilon_t(k, \omega)}{k^4} d\kappa - 1 \right) \quad (9b)$$

to leading nonvanishing order in the quasistatic approximation. Here $k^2 = p^2 + \kappa^2$,

$$\epsilon_l(k, \omega) = 1 + \frac{3\omega_p^2}{k^2 v_F^2} \frac{(\omega + iv) f_l((\omega + iv)/kv_F)}{\omega + iv f_l((\omega + iv)/kv_F)}, \quad (10a)$$

$$\epsilon_t(k, \omega) = 1 - \frac{\omega_p^2}{\omega(\omega + iv)} f_t((\omega + iv)/kv_F), \quad (10b)$$

$$f_l(x) = 1 - \frac{x}{2} \ln(x + 1)/(x - 1), \quad (11a)$$

$$f_t(x) = \frac{3}{2} x^2 - \frac{3}{4} x(x^2 - 1) \ln(x + 1)/(x - 1), \quad (11b)$$

v is the electron collision frequency, $\omega_p = (4\pi n e^2/m)^{1/2}$ is the plasma frequency, and v_F is the Fermi velocity. Although Eqs. (5) are derived assuming locality, it is a convenient fact [12] that these equations are also valid in the nonlocal regime as long as the nonlocal form of the Fresnel coefficients (9) are used.

In Fig. 1, we present the zero-temperature results for the relaxation time T_1 from EWJN for a qubit with an electric dipole moment of magnitude $|e|a_B$, where a_B is the Bohr radius. Both the local and nonlocal results are shown. It is seen that the correct nonlocal dielectric function eliminates the unphysical divergence of $1/T_1$ at $z = 0$. For separations $z \sim \lambda_F$, the differences are very significant, while for $z \gtrsim 10\lambda_F$, the local and nonlocal results nearly coincide. The Fermi wavelength is less than a nanometer, so the transition from local to nonlocal behavior occurs well within the quasistatic regime. It is interesting to note that for the electric-field fluctuations there is a crossover region where the nonlocal result becomes slightly larger than the local result in the range $30\lambda_F < z < 3000\lambda_F$ (see Fig. 1), in alignment with the results of Volokitin and Persson [5], who showed an enhancement of the nonlocal result above the local result. We see that at

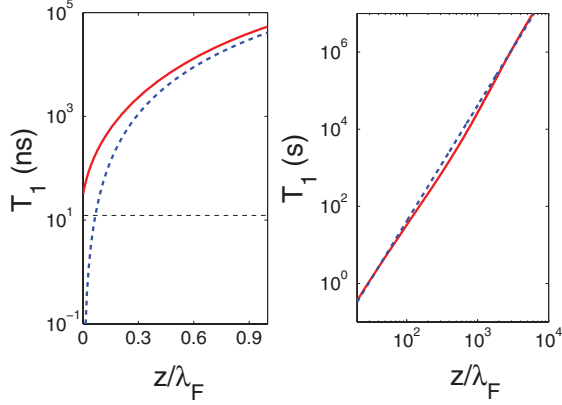


FIG. 1. (Color online) Plot of the T_1 time of a charge qubit computed from Eq. (1) using the local approximation (dashed blue line) and the full nonlocal theory (solid red line). We used the values $E_F = 7$ eV, $\omega = 6\pi \times 10^8$ s $^{-1}$, $\nu = 6\pi \times 10^{12}$ s $^{-1}$, $\omega_p = 1.6 \times 10^{16}$ s $^{-1}$, and $\epsilon = 7.2 \times 10^9 i$, appropriate for a copper surface and a device operating in the GHz range. The dipole moment is taken as $d = |e|a_B$, where $|e|$ is minus the charge on the electron and a_B is the Bohr radius. These results are for zero temperature. The dashed horizontal line in the left plot represents the strength of the electric-field fluctuations inside the bulk of a uniform metal.

$T = 0$ and GHz operations, T_1 from spontaneous emission is of the order of seconds at separations $z \sim 30\lambda_F$. These results are directly applicable to atomic qubits, but the rate $1/T_1$ is proportional to the square of the dipole moment, so rates for other charge qubits are easily deduced.

Figure 2 shows that T_1 falls off slowly at higher frequencies. The divergence of T_1 as $\omega \rightarrow 0$ is removed by including a small finite temperature. Figure 2 is plotted using the local expression, but the nonlocal treatment will give qualitatively similar results.

Figure 3 gives the analogous results for magnetic EWJN on a spin qubit with a magnetic dipole moment of 1 Bohr magneton. Nonlocal corrections are somewhat stronger for this case and persist to larger distances. Interestingly, the

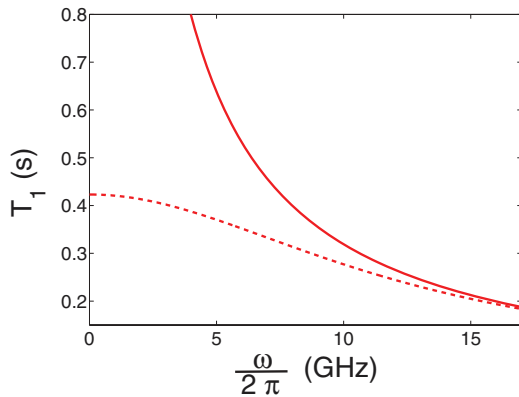


FIG. 2. (Color online) Plot of the T_1 time vs frequency ω of a charge qubit computed from Eq. (1) at different temperatures (solid red line at 0 K and dashed red line at 2 K) at fixed $z = 10\lambda_F$. $E_F = 7$ eV, $\nu = 6\pi \times 10^{12}$ s $^{-1}$, $\omega_p = 1.6 \times 10^{16}$ s $^{-1}$, $\epsilon = 7.2 \times 10^9 i$, and $d = |e|a_B$, as in Fig. 1.

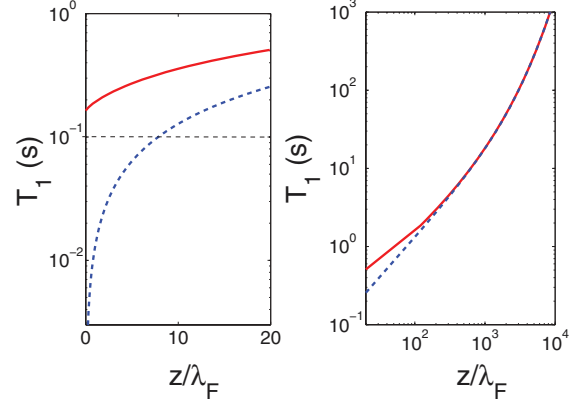


FIG. 3. (Color online) Plot of T_1 time for a spin qubit at zero temperature computed from Eq. (2) in the local approximation (dashed blue line) and the full nonlocal theory (solid red line). $E_F = 7$ eV, $\omega = 6\pi \times 10^8$ s $^{-1}$, $\nu = 6\pi \times 10^{12}$ s $^{-1}$, $\omega_p = 1.6 \times 10^{16}$ s $^{-1}$, and $\epsilon = 7.2 \times 10^9 i$, appropriate for a copper surface and a device operating in the GHz range. We have taken $\mu = \mu_B$, appropriate for a single electron. The rate $1/T_1$ is proportional to the square of μ , so rates for other local magnetic qubits can be easily deduced. The dashed horizontal line in the left plot represents the strength of the magnetic-field fluctuations inside the bulk of a uniform metal.

falloff with distance of T_1 is slower for magnetic EWJN than for electric EWJN. However, magnetic relaxation times are typically somewhat larger than electric relaxation times. The crossover of the local and nonlocal results is not present in the magnetic case. Figure 4 shows that the frequency and temperature dependence of magnetic EWJN is similar to the electric EWJN shown in Fig. 2. Brief mention should be made of the dip that is observed as $\omega \rightarrow 0$ in Fig. 4. The reflection coefficients r_s and r_p both contribute to the magnetic-field fluctuations to the same order in ω/c in the quasistatic approximation. This contrasts with the electric case, where only r_p contributes to leading order in ω/c . The dip is a result of competition between the contributions of r_s and r_p to the field fluctuations. The r_s term in χ_{ii}^B is linear

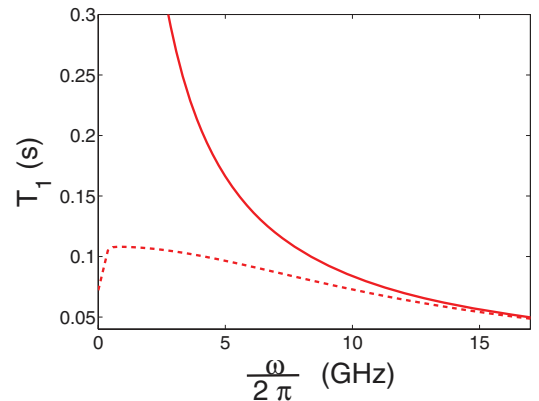


FIG. 4. (Color online) Plot of the T_1 time vs frequency of the spin qubit computed at different temperatures (solid red line at 0 K and dashed red line at 2 K) at fixed $z = 10\lambda_F$. $E_F = 7$ eV, $\nu = 6\pi \times 10^{12}$ s $^{-1}$, $\omega_p = 1.6 \times 10^{16}$ s $^{-1}$, and $\epsilon = 7.2 \times 10^9 i$, appropriate for a copper surface. $\mu = \mu_B$ as in Fig. 3.

in ω as $\omega \rightarrow 0$ and negative, while the r_p term is cubic in ω as $\omega \rightarrow 0$ and positive. We should also mention that for extremely small ω the factor of $\coth(\hbar\omega/2k_B T)$ cancels out the linear ω dependence and the dip flattens out as $\omega \rightarrow 0$ (not observable in the resolution of Fig. 4).

The limit of the nonlocal quasistatic field fluctuations as $z \rightarrow 0$ should be of the same order of magnitude as the value of these fluctuations inside the metal. To check this, we calculate the electromagnetic Green's function inside the bulk of a uniform metal using a nonlocal dielectric function. The result is

$$D_{ij}(\vec{k}, \omega) = \frac{4\pi\hbar}{\omega^2\epsilon_t/c^2 - k^2} \times \left(\delta_{ij} - \frac{c^2 k_i k_j}{\omega^2 \epsilon_l} + \frac{k_i k_j}{k^2 \epsilon_l} (\epsilon_t - \epsilon_l) \right), \quad (12)$$

$$D_{ij}(\vec{r} - \vec{r}', \omega) = \frac{1}{(2\pi)^3} \int d^3\vec{k} e^{i\vec{k}\cdot(\vec{r}-\vec{r}')} D_{ij}(\vec{k}, \omega). \quad (13)$$

Numerical evaluation of (13) when $\vec{r} = \vec{r}'$ gives $D_{xx} = D_{zz} \sim 3.2 \times 10^{-15}$ J s/m. An evaluation of the Green's function outside the metal in the nonlocal quasistatic regime for $z \rightarrow 0$ gives $D_{xx} \sim 1.32 \times 10^{-15}$ J s/m and $D_{zz} \sim 2.6 \times 10^{-15}$ J s/m, slightly less than in the bulk of a uniform metal, as expected.

We see that there are three relevant distance regimes. For $z < 30\lambda_F$, a quasistatic approximation to Henkel's results (5) using the *nonlocal* expressions for r_s and r_p will accurately describe the field fluctuations. For intermediate distances $30\lambda_F < z < \delta/10$ there is a slight enhancement in the electric-field fluctuations of the nonlocal expression compared to the local expression, but in this distance regime the strengths of both electric- and magnetic-field fluctuations are given to reasonable accuracy by their local, quasistatic expressions. For distances $z > \delta/10$, local forms including retardation of the electromagnetic field (5) will accurately describe the field fluctuations.

Comparison of our results with experimental measurements of T_1 times for spin relaxation in single-electron quantum dots supports the notion that relaxation from EWJN may sometimes constitute the dominant relaxation mechanism in present semiconductor qubit architectures. In particular, we reference the low B saturation of T_1 for a single electron in Fig. 4(d) of [15]. In their measurements, T_1 saturates to ~ 40 ms. Plugging their values of $z = 50$ nm and $\hbar\omega_Z = 0.4$ meV into (7b) gives a value of $T_1 \sim 4$ ms. That our expression

gives a shorter relaxation time than what was measured can be understood because we assume the gates constitute a conducting half space, rather than the more sparse gate geometry used in [15]. It is also instructive to compare our results with the measurements of Elzerman *et al.* [16]. They measured a T_1 of 0.55 ms at a magnetic field of 10 T. Using their values of $z = 90$ nm and $\hbar\omega_Z = 0.2$ meV, our results predict $T_1 \sim 15$ ms. While our result is comparable to the measured result, EWJN is clearly not the dominant relaxation mechanism in this situation. Through a perusal of the literature, we have found generally that EWJN is insufficient to describe the spin relaxation rate in experiments with a high external magnetic field.

The density of photon states in a metal is very high owing to the large polarizability. For blackbody radiation, this high density of states does not matter since total internal reflection reduces the outgoing radiation flux to its universal Stefan-Boltzmann value. In contrast, the evanescent waves are strongly enhanced, and the resultant electromagnetic noise just outside the surface can be intense. This is a concern for quantum devices operating close to metallic objects. This Rapid Communication has concentrated on the frequency, temperature, and distance dependence of the noise and on the effects of assuming a local dielectric function. We conclude that the effect is significant for charge qubits with large dipole moments such as double quantum dots. The EWJN relaxation may be the limiting decoherence effect in designs which involve close proximity to bulk metals. For magnetic qubits the effects are smaller, but as can be seen by comparison to [15], they can still be significant. We found that nonlocal effects are very important at short distances; indeed, local calculations can produce spurious divergences. At distances that are large compared to the Fermi wavelength of the metal, local approximations work well.

We have not considered extended qubits for which the off-diagonal function $D_{ii}(\vec{r}, \vec{r}')$ at $\vec{r} \neq \vec{r}'$ is required. This would be the case, for example, in superconducting qubits, for which lossy surface layers can also play a role. We have treated only relaxational decoherence and have ignored the possibility of dephasing. These effects are important for many real devices and can be calculated using similar methods.

We thank M. A. Eriksson, S. M. Girvin, R. McDermott, and F. Wellstood for useful discussions. This work was supported by ARO and LPS Grant No. W911NF-11-1-0030.

-
- [1] E. M. Lifshitz, Zh. Eksp. Teor. Fiz. **29**, 94 (1955) [Sov. Phys. JETP **2**, 73 (1956)].
- [2] G. S. Agarwal, Phys. Rev. A **11**, 230 (1975); **11**, 253 (1975).
- [3] S. M. Rytov, *Theory of Electrical Fluctuation and Thermal Radiation* (Academy of Sciences of the USSR, Moscow, 1953).
- [4] J. B. Pendry, J. Phys. Condens. Matter **11**, 6621 (1999).
- [5] A. I. Volokitin and B. Persson, Rev. Mod. Phys. **79**, 1291 (2007).
- [6] K. Joulain, J.-P. Mulet, F. Marquier, R. Carminati, and J.-J. Greffet, Surf. Sci. Rep. **57**, 59 (2005).
- [7] C. Henkel, S. Pötting, and M. Wilkens, Appl. Phys. B **69**, 379 (1999).
- [8] D. M. Harber, J. M. McGuirk, J. M. Obrecht, and E. A. Cornell, J. Low Temp. Phys. **133**, 229 (2003).
- [9] S. I. Erlingsson and Y. V. Nazarov, Phys. Rev. B **66**, 155327 (2002).
- [10] F. Marquardt and V. A. Abalmassov, Phys. Rev. B **71**, 165325 (2005).
- [11] D. C. B. Valente, E. R. Mucciolo, and F. K. Wilhelm, Phys. Rev. B **82**, 125302 (2010).

- [12] G. W. Ford and W. H. Weber, *Phys. Rep.* **113**, 195 (1984).
- [13] C. Henkel and K. Joulain, *Appl. Phys. B* **84**, 61 (2006).
- [14] E. M. Lifshitz and L. P. Pitaevskii, *Statistical Physics, Part 2*, Course of Theoretical Physics, Vol. 9, Chap. VIII (Pergamon, London, 1980).
- [15] M. Xiao, M. G. House, and H. W. Jiang, *Phys. Rev. Lett.* **104**, 096801 (2010).
- [16] J. M. Elzerman, R. Hanson, L. H. Willems van Beveren, B. Witkamp, L. M. K. Vandersypen, and L. P. Kouwenhoven, *Nature (London)* **430**, 431 (2004).